23rd ABCM International Congress of Mechanical Engineering
December 6-11, 2015, Rio de Janeiro, RJ, Brazil

ESCAPE DYNAMICS IN THE COPENHAGEN PROBLEM

Sheila Crisley de Assis
Maisa de Oliveira Terra
Instituto Tecnológico de Aeronáutica – ITA – Departamento de Matemática, São José dos Campos, SP, Brasil.
sheassis@yahoo.com.br and maisa@ita.br

Abstract. *In this contribution we investigate the escape dynamics in the planar circular restricted three-body problem for the Copenhagen case. This mathematical model describes the planar dynamics of a particle subject to the gravitational potential of two bodies* P_1 *and* P_2*, named primaries, that performs coplanar circular orbits around their center of mass. The mass of third body is much smaller than that of the primaries, thus the movement of* P_1 *and* P_2 *is not disturbed by the third body. The primaries present equal masses, so the mass parameter of mathematical model is 0.5. The necks around* L_2 *and* L_3 *open simultaneously. In this work, we are considering the initial conditions between the collinear Lagrangian points* L_2 *and* L_3*. The analysis is divided into two important cases, which are defined from different energy levels, revealing different possibilities for exists of the accessible regions in the phase space. In the first case, just the neck around* L_1 *is open, then we analyzed trajectories which collide with* P_1 *or* P_2 *and trajectories which not collide until the maximum integration time (limited trajectories); the second case, the necks around* L_2 *and* L_3 *are open, then we have to consider trajectories which collide with* P_1 *or* P_2*, trajectories that escape through* L_2 *and* L_3 *channels and trajectories which not collide or escape from the scattering region after completing the integration time. The spatial distribution of escape time values are also investigated and associated with the fractality of the boundaries. This analysis is valuable both in the context of investigation of natural system and for design of trajectories of modern space missions.*

Keywords: *escape trajectories, space mission design, Copenhagen case and fractal basin boundaries.*

1. INTRODUCTION

An important feature of Hamiltonian systems is that for values of energies below of certain threshold energy, called the *escape energy*, the particles cannot leave the scattering region, but for energies above of the escape energy the trajectories can escape towards infinity through of the open necks. For open Hamiltonian systems there are many investigations in different contexts: Bleher et al. 1988; Ott and Tél 1993; Lai and Tél 2011.

Escape basins can be investigated in open Hamiltonian systems. The escape basins are similar to basins of attraction in dissipative systems. An escape basin is defined as the set of initial conditions which escape of the *scattering region* through of an *exit*. In diagrams of escape basins, each set is plotted by different colors.

There are many papers that studied escape basins: Bleher et al. 1988; Kennedy and York 1991; Poon et al. 1996 and Contopoulos 2002). The analysis about chaotic scattering and escaping orbits in the classical Restricted Three-Body Problem (PR3BP) was investigate in detail by Benet et al 1997, 1998; Nagler 2004, 2005, Davis and Howell 2011, 2012; de Assis and Terra 2013, 2014; Zotos 2015. The analysis of escape dynamic for PR3BP is fundamental in transport processes between different regions in the context of space missions (Sousa-Silva and Terra 2012a, b) and on the study of dynamical evolution of natural systems, involving comets, asteroids and satellites.

For the Copenhagen problem, a specific case of the restricted three-body problem, where the mass parameter of mathematical model equals 0.5 some works can be cited: Nagler 2004 presented a partition of orbits of various types of regular motion, chaotic motion, escape and crash using as scattering region a disk with center at the center of mass and radius equals 10; Gidea and Masdemont, 2007, analyzed the stable and unstable invariant manifolds associated with Lyapunov orbits about the Lagrangian collinear point L_1; Barrio et al. 2008, presented a study using chaos indicators, the crash test and computed the skeleton of symmetric periodic orbits while Zotos 2015 determined the escape basins and crash basins and their corresponding escape/crash times, considering one of the primaries as oblate spheroid.

This contribution aims to investigate the process of escape of trajectories in the context of planar circular restricted three-body problem for the Copenhagen case. Considering the scattering region located between the Lagrangian Point L_2 and L_3. The analysis has been performed for two cases. Namely, in the first situation just the neck around the collinear Lagrangian Point L_1 is open, and, the second situation, all the necks around the three collinear solutions are open. Different basins are available in each case, and several energy levels are considered in order to explore this escape dynamics. In this paper, the primaries are considered as finite bodies.

This paper is organized as follow: in section 2, we present details about the mathematical model; in section 3, the definitions adopted for the escape basins are stated. The numerical results and the conclusion are, respectively, in sections 4 and 5.

2. DETAILS OF THE MATHEMATICAL MODEL

The planar circular restricted three-body problem (PCR3BP) describes the motion of a third body P_3 moving in the gravitational field of two bodies, P_1 and P_2, know by primaries (Szebehely, 1967). The mass of third body is much smaller than the masses of P_1 and P_2, so the motion of primaries is not perturbed by P_3. In the circular version of the model, the orbits of P_1 and P_2 are coplanar circles centered in the barycenter of this 2B system. The P_3 motion is restricted to the plane of motion of the primaries. The mass parameter of this mathematical model is given by $\mu = m_2/(m_1 + m_2)$, with $m_1 > m_2$, while the non-dimensional masses of P_1 and P_2, are given, respectively, by $1-\mu$ and μ. The Copenhagen case, as the masses are equals, $\mu = 0.5$.

The third body's equation of motion are given by

$$\ddot{x} - 2\dot{y} = \Omega_x \quad \text{and} \quad \ddot{y} + 2\dot{x} = \Omega_y \quad \text{, with} \tag{1}$$

$$\Omega(x, y) = \frac{1}{2}(x^2 + y^2) + \frac{1-\mu}{r_1} + \frac{\mu}{r_2} + \frac{\mu(1-\mu)}{2}, \tag{2}$$

$$r_1 = [(x+\mu)^2 + y^2]^{1/2} \quad \text{and} \quad r_2 = [(x - 1 + \mu)^2 + y^2]^{1/2}. \tag{3}$$

The dynamical system has an integration of motion J, the Jacobi constant, given by

$$J(x, y, \dot{x}, \dot{y}) = 2\Omega(x, y) - (\dot{x}^2 + \dot{y}^2) = C. \tag{4}$$

The conservation associated to J defines a three-dimensional invariant manifold in the four-dimensional phase space by

$$\mathcal{M}(\mu, C) = \{(x, y, \dot{x}, \dot{y}) \in \mathbb{R}^4 | J(x, y, \dot{x}, \dot{y}) = C\}. \tag{5}$$

The Jacobi constant C is related with the third body's energy E by $C= -2E$.

This dynamical model has five equilibrium points, called Lagrangian points (Szebehely, 1967), three of these points, known as the collinear points are represented by L_1, L_2 and L_3. These points are unstable and located in the *x-axis*, as shown Fig.1. The Lagrangian point L_1 is located between the primaries; L_2 is on the right of P_2, and L_3 on the left side of P_1. In the Copenhagen case, the Lagrangian points L_4 and L_5 are located in the *y-axis.*

The accessible regions to the trajectories for a given value of C can be obtained by the projection of the surface M in the space of positions (x, y) and imposing $\dot{x}^2 + \dot{y}^2 = 2\Omega(x, y) - C \geq 0$, the Hill regions $\mathcal{M}$ are defined by

$$\mathcal{M}(\mu, C) = \{(x, y) | \Omega(x, y) \geq C/2\}. \tag{6}$$

The boundaries of these regions are called *zero-velocity curves* (zvc). The third body's equations of motion (Eq. (1)) are invariant under the symmetry operation $(x, y, \dot{x}, \dot{y}, t) \to (x, -y, -\dot{x}, \dot{y}, -t)$; while the case for $\mu = 0.5$ has a specific symmetry $(x, y, \dot{x}, \dot{y}, t) \to (-x, -y, -\dot{x}, -\dot{y}, t)$ (Gidea and Masdemont, 2007). In of this case, the necks around the Lagrangian points L_2 and L_3 open simultaneously to same value of C.

In Fig.1 is shown four possible cases of Hill's regions for the Copenhagen case. The white regions represent the Hill's region; the gray regions indicate the forbidden regions and the black line represent the *Zero Velocity Curves (ZVC).* The symbols *x* (plotted in red color) represent the five Lagrangian points, while the black points represent the primaries P_1 and P_2. In case (a), $C > C_1$, no transfer orbits between the primaries are possible. In case 2, $C_1 > C > C_{2,3}$ there are only internal transfers, while in the cases (c) and (d) ($C_{2,3} > C$), internal and external connections are possible.

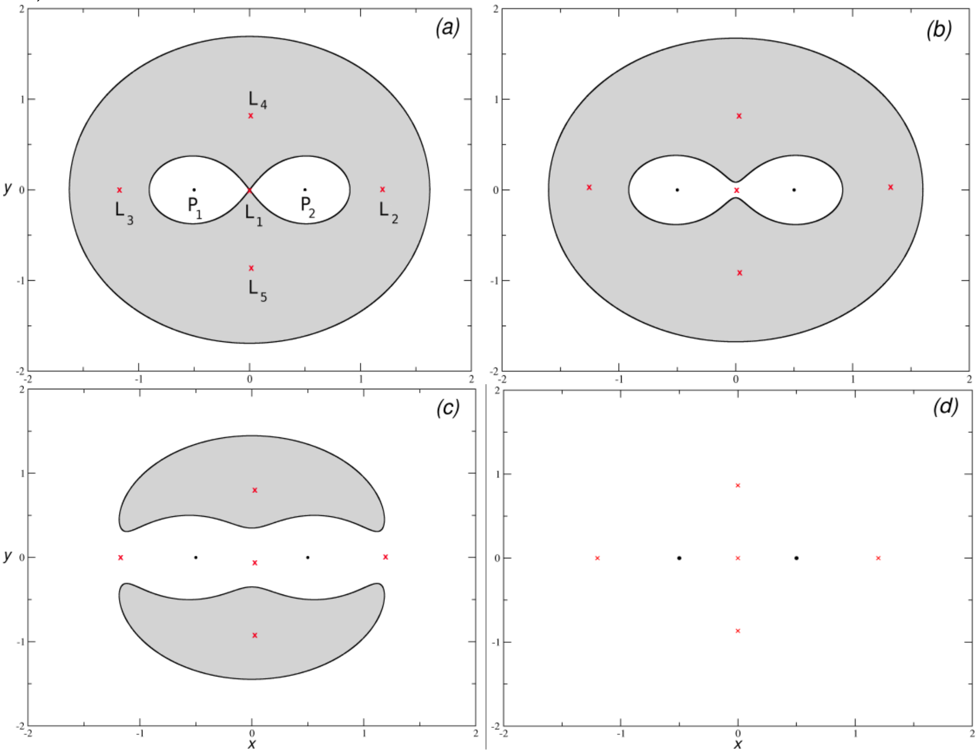

Figure 1. Four possible cases Hill's regions for the Copenhagen case.

3. DEFINITIONS OF THE ESCAPE BASINS

In this contribution, we analyze escape basins, fractal basins boundaries and escape and collisional time for Copenhagen case ($\mu = 0.5$). The set of initial conditions is defined in a *scattering region* between the Lagragian collinear points L_2 and L_3. As in this work the primaries are considered as finite bodies, we analyzed five behaviors of trajectories, originating five different basins*: the bounded basin*, corresponding to trajectories which remain in the scattering region until a maximum integration time t_f (the maximum integration time adopted was 200 dimensionless time unit (*dtu*)), *the basin by L_2*, constituted by trajectories which escape through the neck around L_2; *the basin by L_3* with trajectories which escape through open neck around the L_2; basin of trajectories that collide with P_1 (*collision 1 basin*) and basin of trajectories that collide with P_2 (*collision 2 basin).* In the escape basin diagrams, the basins mentioned above are represented, respectively, by colors yellow, green, blue, black and red.

Our analysis was divided in two different regions defined according with Jacobi constant values:

- **Region I:** $(C_1 > C > C_{2,3})$ only the neck around L_1 is open, so, we have the sets *bounded, collision 1 and collision 2.*
- **Region II**: $(C_{2,3} > C)$ the necks around L_1, L_2 and L_3 are open, so in this situation, we have the five behaviors of trajectories analyzed.

For each region results are presented for different Jacobi constant *C* and scaled mean radius values. The scaled mean radius can be obtained by (Hamilton and Burns, 1991 and Davis and Howell, 2012)

$$R_H = \left(\frac{R_{P_k}}{d_{P_1P_2}}\right) / \left(\frac{\mu}{3}\right)^{1/3} \quad (6)$$

Where $d_{P_1P_2}$ denotes the distance between the two primaries P_1 and P_2, and R_{P_k} is the mean radius (as in this work we are considering both primaries with the same radius value, k can be 1 or 2). In this paper we consider three distinct groups according to R_H values. As a representative case of Group A, we choose $R_H = 8.215805403\, x\, 10^{-3}$; for Groups B and C we chose, respectively, the following values $R_H = 5.5058633x\, 10^{-2}$ and $R_H = 5.5058633x\, 10^{-1}$.

The escape basins were computed in a three-dimensional manifold fixing the value of Jacobi constant *C*. We consider a grid of about 1600x1300 initial conditions in the Poincaré section defined by the *(x, y)* plane, for $\dot{x} = 0$ and $\dot{y} > 0$, with $x_{L_3} \leq x \leq x_{L_2}$ and $-6.0 \leq y \leq 6.0$.

4. ESCAPE BASINS RESULTS

4.1- Results for Region I: ($C_1 > C > C_{2,3}$)

In this region, just the neck around L_1 is open, allowing the communication between the regions of P_1 and P_2. Figure 2 displays the Poincaré section (Fig. 2(a)) and escape basins (Fig. 2(b), (c) e (d)) for Copenhagen case with set of initial conditions located between the Lagragian points L_2 and L_3 for *C=4.248*. The Figs. 2 (b), (c) and (d) exhibit, respectively, results for groups A, B and C, defined above. The Poincaré plot is rich in details. We observed two large stability regions located one on the left of P_1 and other between L_1 and P_2. We can see other smaller stability regions, immersed in chaotic sea in different regions of diagram. Fig. 2 (b) has more initial conditions bounded than in the other cases, while Fig. 2 (c) presents fractal basin boundaries around some stability islands immersed in the chaotic sea. These fractal basin boundaries are associated with long escape time, revealing high sensitivity to initial conditions (de Assis and Terra 2014). In Fig. 2 (d), there is just initial conditions that collide with P_1 and P_2, respectively, plotted in colors black and red.

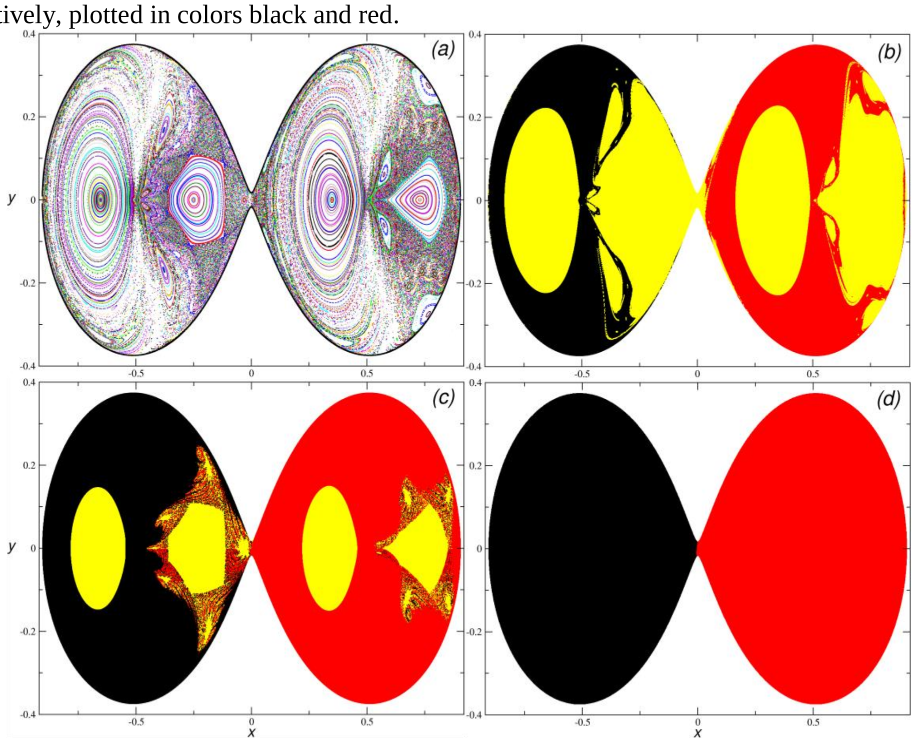

Figure 2. Results of Poincaré section (a) and escape basins for Group A (b), Group B (c) and Group C (d) for *C=4.248*.

When the C value is reduced to *4.0* (Fig. 3), the neck around L_1 is even more open than in the previous case. The two large stability regions remain, while the smaller islands disappeared or are very small. The chaotic sea dominates almost all the phase space. Now, we observed fractal basin boundaries in the results for Group A (Fig. 3(b)), in the region of chaotic sea where are the longest escape time. The diagrams for Group B and Group C present more regions with smooth boundaries than the results for Group A. The escape basin for Group C (Fig. 3 (d)) continues to present only collisional initial conditions.

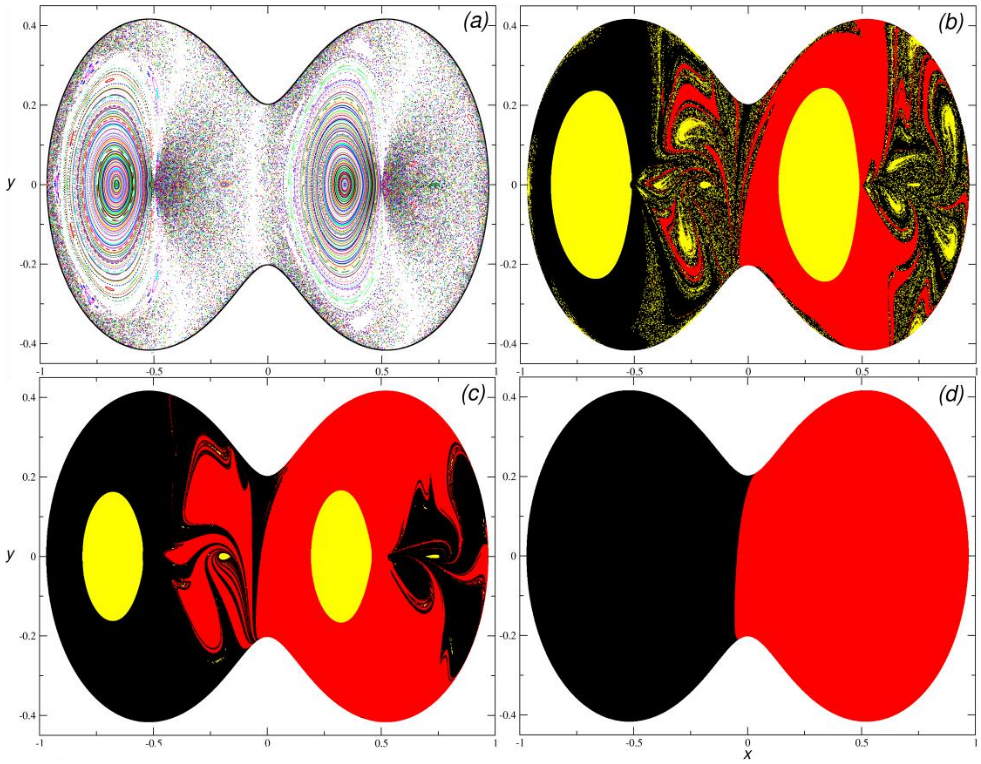

Figure 3. Poincaré section (a) and escape basins for Group A (b), Group B (c) and Group C (d) for *C=4.0*.

4.2- Results for Region II: $(C < \boldsymbol{C_{2,3}})$

The necks around Lagrangian points L_1, L_2 and L_3 are open. In this situation, we analyzed the five behaviors of trajectories defined in Section 3. Figure 4 shows the results of Poincaré section (Fig. 4(a)) and escape basins for Groups A (Fig. 4(b)), B (Fig. 4(c)) and C (Fig. 4(d)) for *C=3.7*. We can see by Poincaré plot that the chaotic sea involves a big region of the space phase and the two stability regions located on the left of P_2 and between L_1 and P_2 are smaller. In planar circular restricted three-body problem, stability islands can appear or disappear when we change the Jacobi constant. The collisional sets with P_1 and P_2 contain together, almost 75%, 84% and 97% of total considered initial conditions, respectively, for Groups A, B and C. In diagram of Group A, there are a lot of initial conditions belonging to escape basins by L_2 and L_3 that are spread over the diagram, forming fractal basin boundaries. The fractal basin boundaries coincide with the stable manifold of a chaotic saddle. In diagram of Group C, we can see initial conditions that belong to collision 1 basin on the right P_2, this fact was not noted in previous cases.

When we analyze results of escape basins for C=3.67 (Fig. 5), we can realize that the sizes of escape basins by L_2 and L_3 are larger if compared with the previous case. Through the Poincaré section, we can detach the presence of two big stability islands observed since the beginning of our analysis and the chaotic sea domain. Fig. 5 (b) presents more regions with fractal basins boundaries than the results present in the Figs. 5 (c) and (d). The escape basin by L_2 and L_3 contain together, almost 16%, 12% and 4% of total considered initial conditions, respectively, for Groups A, B and C. When we reduce the values of C, the escape times and collisional times become shorter and the basins boundaries become smoother.

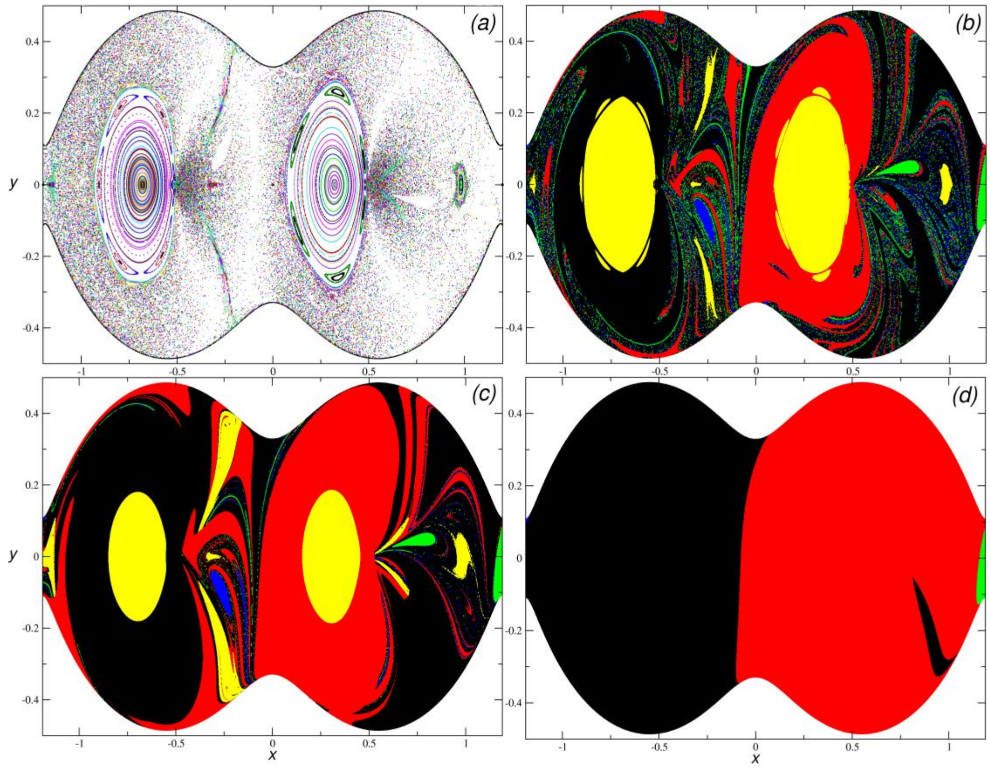

Figure 4. Poincaré section (a) and escape basins for Group A (b), Group B (c) and Group C (d) for C=3.7.

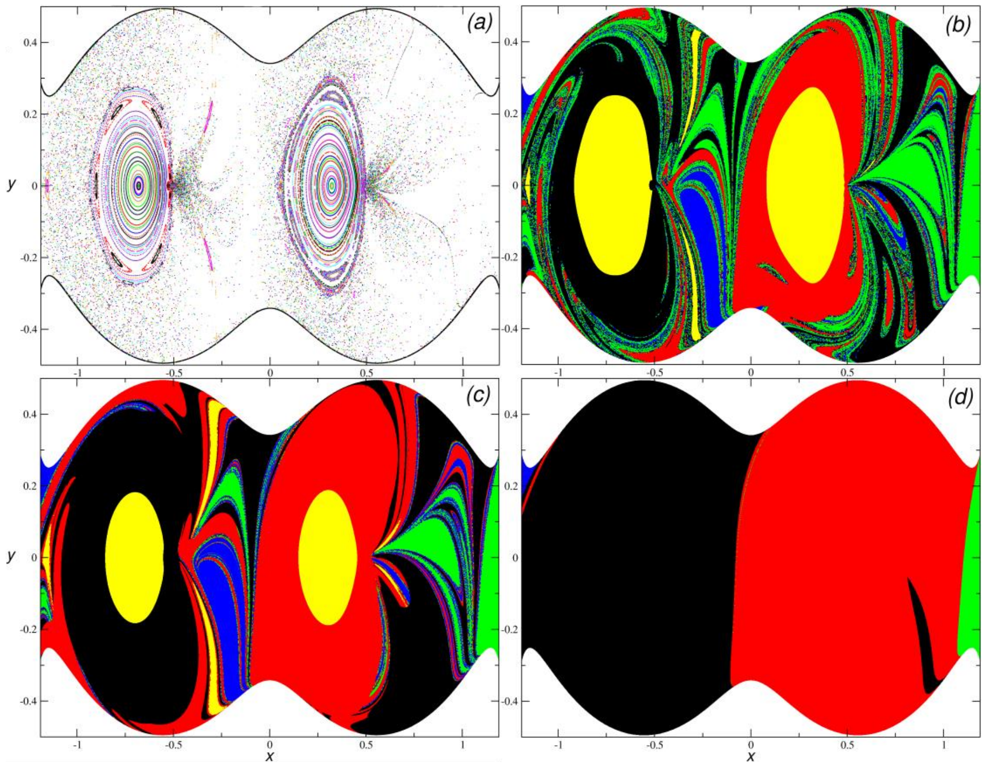

Figure 5. Poincaré section (a) and escape basins for Group A (b), Group B (c) and Group C (d) for *C=3.67*.

4.3- One overview analysis

In this part of the paper, we present an overview analysis of the escape problem for Copenhagen case for the groups A, B and C defined above through of the percentage of solutions of each basin analyzed as function of the Jacobi constant for fixed t_f = *200 dtu* (Fig. 6). In these diagrams, we adopted the same color code defined in the section 3. The dashed vertical line indicates the critical values for $C_{2,3}$.

Frame (a) of Fig. 6 exhibits results for Group A. At the beginning this analysis (higher values of C), the *bounded basin* has more than 50% of the total considered initial conditions, and at the end (smaller values of C), this set has approximately 9% of initial conditions. The two collisional basins present increase in the number of initial conditions until $C = C_{2,3}$; after we observed decrease of percentage. The escape basin by L_2 and L_3 contain together, almost 70% of initial conditions at the end of interval.

In Group B (Fig. 6 (b)), the collisional basins begin the analysis with almost 40% of initial conditions each one, while that bounded basin present approximately 23% of initial conditions. At the end of interval, the percentage of initial conditions of escape basins by L_2 and L_3 and collisional sets with P_1 and P_2 are between 20% and 30%. In the third case (Group C), throughout the interval, the collisional sets have the greatest percentages. At the end of interval, the escape basin by L_2 has approximately 20% of initial conditions, while that escape basin L_3 has approximately 10%. In this case, we do not observe trajectories bounded.

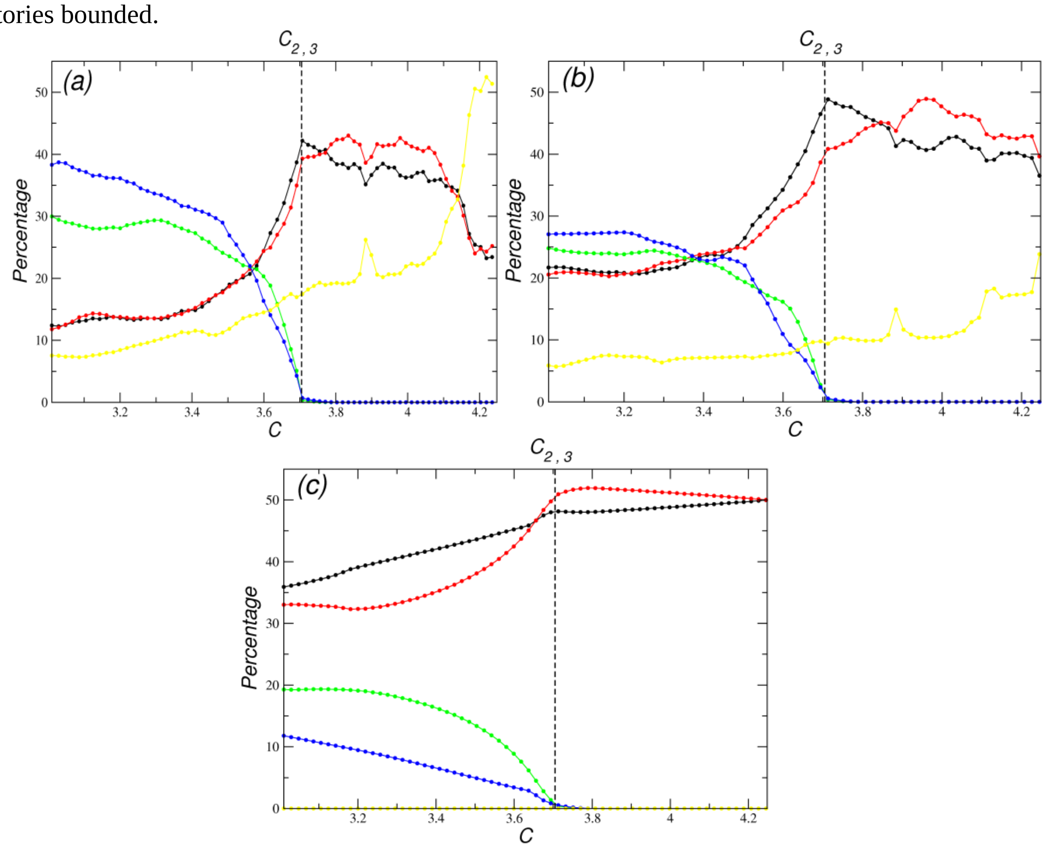

Figure 6. Percentage of initial conditions of each considered basin as a function of C for (a) Group A; (b) Group B and (c) Group C. The dashed vertical line indicates the critical values of C.

5. CONCLUSIONS

In this contribution the escape dynamics of a third body in a scattering region between the Lagragian collinear points L_2 and L_3 was investigated for the planar circular restricted three-body problem for the Copenhagen case. The analysis is divided into two import cases, which are defined from different energy levels, reveling different possibilities of exits of the accessible regions in the phase space. We considered five different behaviors to trajectories: *(i)* and *(ii)* trajectories which collide with the mean radii established for the primaries P_1 and P_2; *(iii)* and *(iv)* trajectories which escape scattering region through the necks around L_2 and L_3 and *(v)* trajectories which not collide or not escape from scattering region after completing the integration time. We showed that fractality of the basin boundaries in this dynamical system presents a strong dependence with the Jacobi constant and with scaled mean radius represented by R_H. These analyses are fundamental in the context of investigation of natural systems and for design of trajectories of modern space missions.

6. ACKNOWLEDGMENTS

The first author is supported by Capes (Brazil). Both authors are thankful to FAPESP (Grant 12/21023-6).

7. REFERENCE

Barrio, R., Blesa, F., Serrano, S., 2009. "Periodic, escape and chaotic orbits in the Copenhagen and the (n+1)-body ring problems." Commun. Nonlinear Sci. Numer. Simulat., Vol. 14, pp. 2229-2238.

Bleher, S., Grebogi, C., Ott. E., Brown, R., 1988. "Fractal boundaries for exit in Hamiltonian dynamics." *Phys. Rev. A.* Vol. 38(2), pp. 930-938.

Benet, L., Trautmann, D., Seligman, T. H., 1997. "Chaotic scattering in the restricted three-body problem i. The Copenhagen problem." Celest. Mech. Dyn. Astron., Vol 66, pp. 203-228.

Benet, L., Trautmann, D., Seligman, T. H., 1998. "Chaotic scattering in the restricted three-body problem ii. Small mass parameter." Celest. Mech. Dyn. Astron., Vol 71, pp. 167-189.

Contopoulos, G., 2002. "Order and chaos in dynamical astronomy." *Springer,Berlin.*

Davis, D. C., Howell, K. C., 2011. "Trajectories evolution in the multi-body problem with applications in the Saturnian system." Act. Astronaut, Vol. 69, pp. 1038-1049.

Davis, D. C., Howell, K. C., 2012. "Characterization of trajectories near the smaller primary in restricted problem for applications." *Journal of Guidance, Control and Dynamics*, Vol. 35, pp. 116-128.

de Assis, S. C., Terra, M. O., 2013. "Biparametric analysis of the escape dynamics in the Solar System: some preliminary results." *22nd. International Congress of Mechanical Engineering (COBEM 2013), Ribeirão Preto – SP.*

de Assis, S. C., Terra, M. O., 2014. "Escape dynamics and fractal basin boundaries in the planar Earth-Moon system." *Celestial Mechanics and Dynamical Astronomy*, Vol. 120, pp. 105-130.

Gidea, M., Masdemont, J., 2007. "Geometric of homoclinic connections in a planar circular restricted three body problem". *International Journal of Bifurcation and Chaos*, Vol. 17, pp. 1151-1169.

Hamilton. D. P., Burns, J. A., 1991. "Orbital stability zones about Asteroids." *Icarus*, Vol. 92, pp. 118-131.

Kennedy, J., Yorke, J. A., 1991. "Basins of Wada." *Phys. D*, Vol. 9, pp. 213-225.

Lai, Y. C., Tél, T., 2011. "Complex Dynamics on Finite Time Escape." *Springer, New York.*

Nagler, J., 2004. "Crash test for the Copenhagen problem." *Physical Review E*, Vol. 69, pp. 066218.

Nagler, J., 2005. "Crash test the restricted three-body problem." *Physical Review E*, Vol. 71, pp. 026227.

Ott, E., Tél, T. 1993. "Chaotic scattering: an introduction." *Chaos*, Vol. 3(4), pp. 417-426.

Poon, L., Campos, J., Ott. E., Grebogi, C."Wada basin boundaries in chaotic scattering." *Int. J. Bifurc. Chaos*, Vol. 6, pp. 251-266.

Sousa-Silva, P. A., Terra, M. O., 2012a. "Applicability and dynamical characterization of the associeted sets of the algorithmic weak boundary in the lunar sphere of influence." *Celestial Mechanics and Dynamical Astronomy*, Vol. 113, pp. 141-168.

Sousa-Silva, P. A., Terra, M. O., 2012b. "Diversity and validity of stable-unstable transitions in the algorithmic weak stability boundary." *Celestial Mechanics and Dynamical Astronomy*, Vol. 113, pp. 453-478.

Szebehely, V., 1967. "Theory of Orbits". *Academic Press*, New York.

Zotos, E. E., 2015. "Crash test for the Copenhagen problem with oblateness." *Celestial Mechanics and Dynamical Astronomy*, Vol. 122, pp. 75-99.

8. RESPONSIBILITY NOTICE